

A Novel Inkjet Printed Carbon Nanotube-Based Chipless RFID Sensor for Gas Detection

Arnaud Vena^{#1}, Lauri Sydänheimo^{#2}, Manos M. Tentzeris^{*3}, Leena Ukkonen^{#4}

[#]*Department of Electronics, Rauma Research Unit
Tampere University of Technology, Finland*

¹arnaud.vena@tut.fi

²lauri.sydanheimo@tut.fi

⁴leena.ukkonen@tut.fi

^{*}*School of ECE, Georgia Tech
Atlanta, GA 30332-250, USA*

³etentze@ece.gatech.edu

Abstract— This paper presents a fully inkjet printed wireless chipless sensor for carbon dioxide detection. It is composed of two split ring resonators 90 degrees rotated to each other for a total size of 18x46 mm². The first resonator is used for gas detection whereas the second provides identification of sensor, and a reference for accurate detection. The conductive part of the sensor is realized with silver ink, and the sensitive part is composed of carbon nanotube-based ink. The detection principle relies on a dual-polarization frequency-stepped continuous wave radar operating in the ISM band from 2.4 GHz to 2.5 GHz. Simulations and measurements both wireless, and with a transmission line, they validate the concept.

I. INTRODUCTION

Nano-particles based sensors have been studied over the past recent years because they feature unbeatable sensitivity to physical parameters and quick response time. The industrial and environmental sectors are looking for new inexpensive solution to track hazardous chemicals at volume scale. Besides, wireless and battery-less radio-frequency-identification (RFID) sensors [1]-[2] attract a growing interest because they feature a superior lifetime so that maintenance cost is dramatically reduced. Further, the installation of a large network of RFID sensors is more flexible and can be done with less effort, in comparison with a wired sensor network. In some special cases, conventional RFID sensors or active wireless sensor cannot be used. For example, when the operating temperature range is over the range of the chip, or when the environment is subject to electro discharges or a hazardous level of radiation. In this special case, chipless sensors [3]-[4] are more robust, and can still work above hundreds of degrees until the substrate or the conductor itself is damaged. Chipless sensors operate in a totally different way compared to conventional RFID sensors. From the detection system point of view, they are seen as static radar target reflecting every time the same electromagnetic response when submitted to the same incident wave as shown in Fig. 1. A chipless sensor is only composed with conductive strips and sensitive materials or components, so that no chip IC is required. A very low cost unit can be achieved because it can be fully realized with printing technique.

Nanoparticle-based sensors have shown a high sensitivity to different molecules even for very small concentrations. It is shown that nanoparticle-based materials are efficient even when deposited in thin films [3]-[5]. The materials that have been studied for their sensing properties are CNTs [3], graphene [5] and silicon nanowires [4]. The detection of CO₂, NO_x, Ammonia [3] [5], humidity [4], as well as temperature, are often mentioned. In every case, the required behavior is to obtain a complex permittivity change as a function of concentration of a chemical.

This paper proposes a novel chipless sensor design to detect the presence of carbon dioxide in the air. To make it sensitive to this molecule, we deposited a thin layer of carbon nanotubes embedded in PEDOT-PSS solution. The full tag is realized with an inkjet printer, so that, both conductive silver ink and CNT-based PEDOT-PSS ink are printed on flexible laminate. The final realized sensor achieves a very low unit cost and doesn't need any additional operations to work, contrary to a conventional RFID sensor. The chipless sensor operates in the ISM band at 2.45 GHz, so that a large transmitting power can be used, and potential long read range

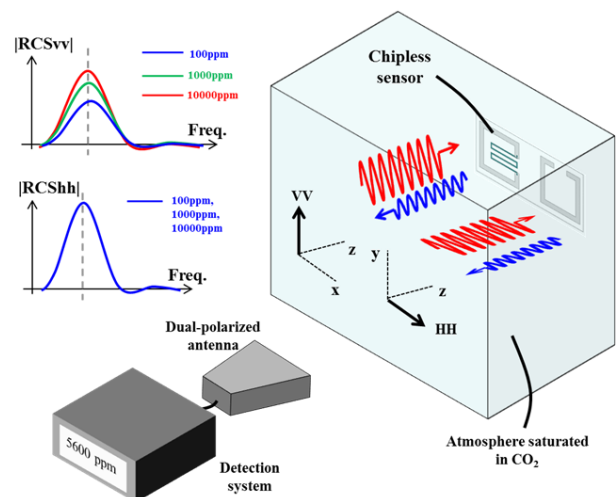


Figure 1. Principle of wireless detection of gas concentration with a chipless sensor.

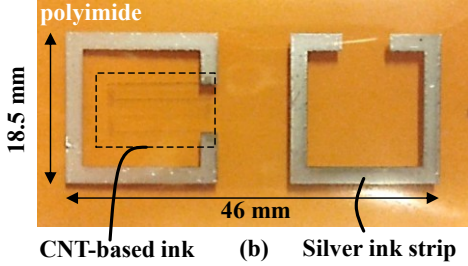
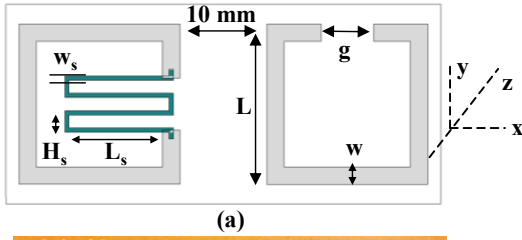


Figure 2. (a) Layout of the chipless sensor designed under CST Microwave Studio. (b) View of the fully inkjet printed sensor. The dimensions are provided in Table I. The transparent CNT-based ink deposit is located within the left scatterer.

can be achieved compared to chipless sensors operating in the UWB band. The sensor reflects a different response depending on the polarization. It allows creating a “static” magnitude reference in one polarization whereas in orthogonal polarization, the response is correlated with the physical parameter change as depicted in Fig. 1. Besides, depending on the resonant frequency of the reference response, a specific ID can be affected to a given sensor.

The section II will present the sensor design and operating principle. Then the section III provides details concerning the measurement setup and the results validating the design before concluding.

II. SENSOR PRINCIPLE AND DESIGN

A. Sensor Design

The mean to extract the sensed parameter as well as the sensor identifier in a chipless sensor is fundamentally different to compare with a conventional RFID sensor. The absence of chip IC prevents the use of any transmission protocol as it is the case for a classical modulation scheme. For a chipless sensor, the ID and the gas concentration extraction relies upon the static backscattered response in frequency-domain [4] or in time-domain. We propose in this paper a sensor for which the electromagnetic response is frequency encoded. The sensor of the Fig. 2 (a) and (b) has been designed to operate in the 2.45 GHz ISM band. It is based on dual-split ring resonator (SRR) 90 rotated to each other. The squared SRR shape has already been used in [6] for a different purpose. This shape allows for miniaturization with a factor two compared to a closed loop. Further, the resonant frequency can be tuned depending of the gap length, providing an additional flexibility. The two SRRs have the same dimensions, provided in Table I. A separation of 10 mm between the two SRR is enough to limit the coupling effect. The conductive strip width $w=2\text{mm}$ is chosen to ensure good radiating performances even with silver ink conductivity that

TABLE I. SENSOR'S DIMENSIONS IN MM

Sensor ID	L	g	W	L_s	W_s	F_0
1	18.25	6	2	12	0.75	2.5 GHz
2	18.5	6	2	12	0.75	2.45 GHz
3	18.75	6	2	12	0.75	2.4 GHz

is 10 to 100 times inferior compared to bulk conductor. The tag shown in Fig. 2 (b) has been inkjet printed on polyimide substrate ($\epsilon_r = 3.5$, $\tan\delta = 0.0027$). The conductive strip consists of 2 layers of silver ink (Harima Nanopaste) printed at 635 dpi, followed by a sintering at 150°C during 90 minutes. The gap g allows the insertion of the sensitive strip with a length at least equal to 6 mm. The first reason is to get a relative high resistance value, to avoid shorting the scatterer and cancel the resonant peak. The second reason is to allow for the increase of the sensitive surface. Indeed, we can consider an initial sheet resistance of $1000 \Omega/\text{sq}$, with two printed CNT ink layers. To modify the resistance of the strip we can either modify the width or the length of the strip. However, to achieve a same resistance value, it is more judicious to increase both the width and the length of the strip. As a result, the strip's surface is maximized. The scatterer denoted 1 in Fig. 2 (b) contains the sensitive material in its gap. It reflects an electromagnetic response correlated with the sensed parameter, when impinged by a vertical-polarized incident wave. The scatterer denoted 2, with no sensitive material, reflects always the same response to an incident horizontally-polarized wave. Its purpose is to provide, first, a magnitude reference to enhance the sensing accuracy. Second, it provides the ID of the sensor, which depends on its resonant frequency.

B. Behavior of CNT-based ink

In the gap location, the electric field is at its maximum so that a sensitive material could be judiciously placed in this area to create a sensor. Indeed, if the relative permittivity of the material is modified, the effective permittivity “seen” by the scatterer is also modified, and a resonant frequency shift could be recorded. Further, if the conductivity of the material is modified, it will affect the losses of the scatterer, and the reflected signal strength as well as the bandwidth of the resonant peak. For this study, we used the single-walled CNT (SWCNT) embedded in PEDOT – PSS ink from Polyink company [7]. It presents a large conductivity change when subject to gas, temperature as well as humidity. The physical explanation is due to the adsorption of certain molecules by the CNT, creating holes in the conductive band [8]. Figure 3 (a) shows radar cross section (RCS) simulation results for the design presented Fig. 2 (a), when the sheet resistance of the sensitive strip R_s is varied from $1000 \Omega/\text{sq}$ to $4000 \Omega/\text{sq}$. We clearly observe an amplitude variation depending on the sheet resistance value in vertical polarization. Meanwhile, the RCS in horizontal polarization is not modified at all. This confirms that the electromagnetic response in horizontal polarization can be used as a magnitude reference for the sensed parameter.

C. Generation of an Identifier

In Fig. 3 (b), one can observe that, the resonant frequency of the peak in horizontal polarization varies from 2.4 GHz to 2.5 GHz, depending on the dimension L . As shown in Table I, a simple way of coding is to associate an ID to a specific resonant frequency. Thus, for $L=18.25$ mm, the associated resonant frequency of 2.5 GHz provides the ID 1, whereas for $L=18.5$ mm and $L=18.75$ mm, the sensor IDs are 2 and 3, respectively. It is noteworthy that the resonant frequency, so the ID, is independent of the RCS variation in vertical polarization due to gas concentration change as previously shown in Fig. 3 (a).

III. VALIDATION OF THE SENSOR

We implemented a frequency-stepped continuous wave radar (FSCW) technique to measure the RCS variation of the chipless sensor. For this purpose, we used a Vector Network Analyzer (VNA) as main equipment because it embeds a CW source able to produce a frequency sweep and a power detector in the receiving path. The two ports of the VNA are connected to a dual-polarization wideband antenna ETS Lindgren 3164-04 (shown in Fig. 4 (a)) having a gain of 9 dBi around 2.45 GHz. The record of the parameter S_{11} and S_{22} provide indirectly the RCS responses in vertical and

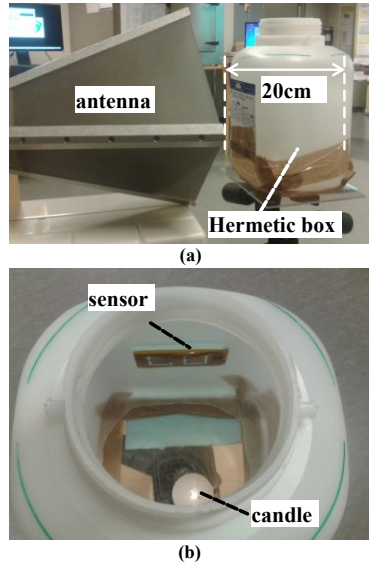


Figure 4. (a) View of the FSCW radar measurement set-up (b) Inner view of the plastic receipt containing the chipless sensor and the candle used to saturate the air in CO_2 .

horizontal polarization, respectively. The calibration for the RCS extraction is described in [9] and relies on three measurements as follows:

- First, the background is measured with no sensor. It allows the extraction of the clutter map of the measurement environment.
- Second, a known reference target such as a rectangular plate is placed at the location where the sensor will be detected. This measurement allows taking into account all the filtering effect due to the antenna, cable and free space channel.
- Third, the sensor itself is measured.

To measure the relationship between CO_2 concentration and RCS variation, the chipless sensor is placed inside a hermetic plastic box 20 cm away from the antenna aperture as shown in Fig. 4 (a) and (b). To increase the level of CO_2 slowly in order to monitor the concentration change, a candle was used. The candle flame burns the oxygen and the wax made of hydrocarbons, when switched on. In turn, it creates mostly CO_2 , and a little water. When the candle turns off, the CO_2 concentration reaches its maximum value.

Figures 5 (a) and (b) show the measured RCS of the sensor of the Fig. 2 (b), during a cycle of candle burning in a hermetic box in vertical and in horizontal polarization, respectively. In the step denoted “1” in Fig. 5 (a), the candle flame starts burning oxygen. The step “2” is corresponding to the candle switch off event due to the lack of oxygen, whereas the step “3” refers to the end of the record. One can see a significant increase of the RCS value close to 1 dB from the initial time to the end of the experiment. It is to be noted that level of RCS is still increasing after the candle switched off, showing the response time of the sensor. Meanwhile, the record of the horizontal polarization response that comes from the SRR with no sensitive material doesn’t show any significant variation. This confirms that the horizontal polarization response can be used for reference purpose, if the

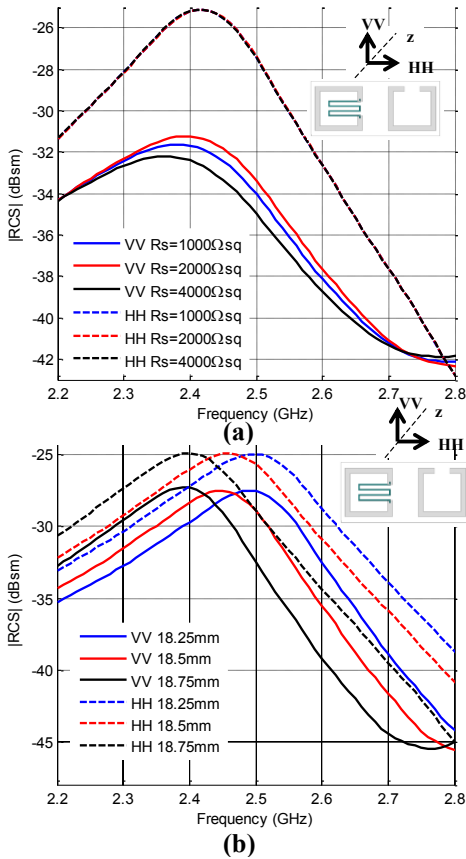


Figure 3. (a) RCS simulation results for $L=18.5$ mm, when the sheet resistant of the sensitive meandered strip R_s shown in Fig. 2 (a) and (b) is varied. (b) RCS simulation results for several length L in both polarizations. The dimensions of the sensor are provided in Table I.

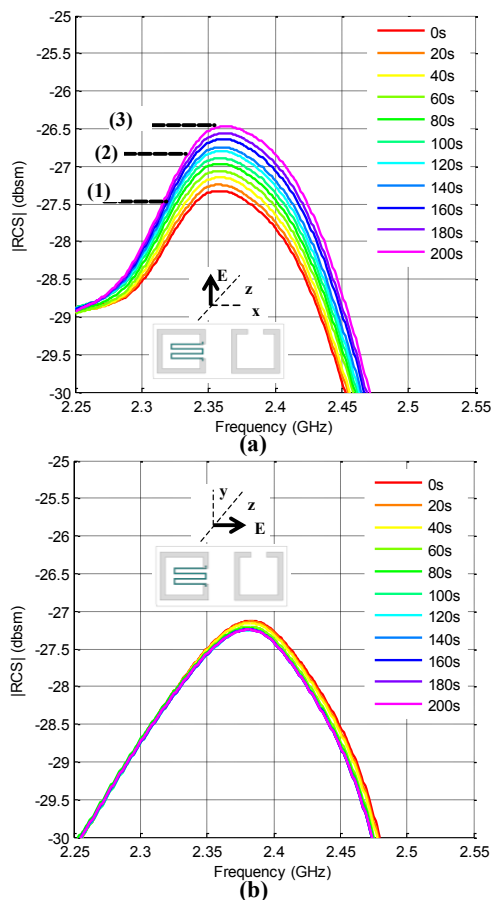


Figure 5. RCS measurement results for the sensor with ID 2 ($L=18.5$ mm) subject to CO_2 (a) in vertical polarization (b) in horizontal polarization. A measurement is recorded every 20s to monitor the CO_2 concentration rising.

sensor has to be read for several detection distances. Indeed, whatever the detection distance the normalized magnitude difference between the orthogonal electromagnetic responses remains the same. One can see that the resonant frequency is below 2.4 GHz. Indeed, the sensor is applied on object having a significant thickness to compare with its thin polyimide substrate. As a result, the effective permittivity rises. Figure 6 shows RCS measurement results in free space in horizontal polarization for sensors of different length. The resonant frequency can be clearly extracted from 2.4 to 2.5 GHz, so that for each one, a different ID can be associated.

IV. CONCLUSIONS

This paper confirms the possibility to use a fully printed chipless RFID sensor for carbon dioxide detection through a dielectric box. The polarization diversity of the presented design allows combining an accurate sensor with an identification function. The wireless measurements have revealed a good CO_2 sensitivity with 1 dB of RCS shift from a low concentration to a large concentration. This confirms that the designed sensor is well sensitive to CO_2 . However, CNT-based sensors are not known to be selective to only one chemical species. A possible solution to address this issue is

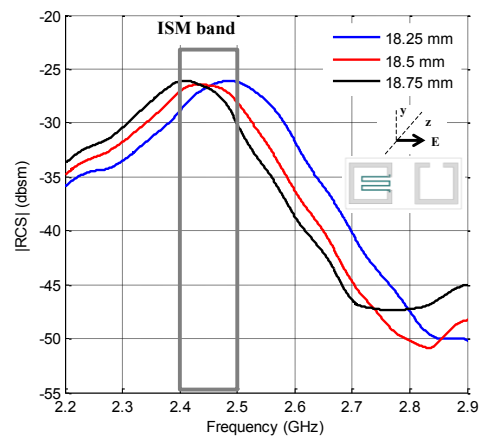


Figure 6. (a) Free space RCS measurement result in horizontal polarization for different length L . The dimensions of sensors are provided in Table I.

to use functionalized CNTs. A future study could focus on the use of several functionalized CNTs to realize a CO_2 sensor that may avoid false alarms. The study of the repeatability of the sensor behavior and its reproducibility will also be investigated.

ACKNOWLEDGMENT

This research has been funded by Finnish Funding Agency for Technology and Innovation, Academy of Finland and Centennial Foundation of Finnish Technology Industries. The authors also acknowledge the NEDO Japan and the NSF.

REFERENCES

- [1] K. Finkenzerler, "Rfid handbook: fundamentals and applications in contactless smart cards, radio frequency identification and near-field communication" Wiley. 2010.
- [2] S. Manzari, C. Occhiuzzi, S. Nawale, A. Catini, C. Di Natale, G. Marrocco, "Polymer-doped UHF RFID tag for wireless-sensing of humidity," IEEE Int. Conf. on RFID, Orlando, April 2012, pp. 124-129.
- [3] L. Yang, D. Staiculescu, R. Zhang, C.P. Wong, M.M. Tentzeris, "A novel "green" fully-integrated ultrasensitive RFID-enabled gas sensor utilizing inkjet-printed antennas and carbon nanotubes," IEEE APSURSI, pp.1-4, 1-5 June 2009.
- [4] A. Vena, E. Perret, S. Tedjini, D. Kaddour, A. Alexis and T. Barron, "A compact chipless RFID tag with environment sensing capability," IEEE MTT-S Int. Microwave Symposium Digest, 2012, 17-22 June 2012.
- [5] L. Taoran, V. Lakafosis, L. Ziyin, C.P. Wong, M.M. Tentzeris, "Inkjet-printed graphene-based wireless gas sensor modules," IEEE 62nd Electronic Components and Technology Conference (ECTC), pp.1003-1008, May 29 2012-June 1 2012.
- [6] H-S Jang, W-G Lim, K-S Oh, S-Mo Moon and J-W Yu, "Design of Low-Cost Chipless System Using Printable Chipless Tag With Electromagnetic Code," IEEE Microwave and Wireless Components Letters, vol.20, no.11, pp.640-642, Nov. 2010.
- [7] A. Denneulin, J. Bras, A. Blayo, B. Khelifi, F. Roussel-Dherbey & C. Neuman, "The influence of carbon nanotubes in inkjet printing of conductive polymer suspensions," Nanotechnology, vol. 20, no. 38, p. 385701, 2009.
- [8] Y. Wang and J. T. W. Yeow, "A Review of Carbon Nanotubes-Based Gas Sensors," Journal of Sensors, vol. 2009, Article ID 493904, 2009.
- [9] A. Vena, E. Perret, S. Tedjini, "Design of Compact and Auto-Compensated Single-Layer Chipless RFID Tag," IEEE Trans. on Microwave Theory and Techniques, vol.60, no.9, pp.2913-2924, Sept. 2012.